COMMUNICATIONS IN NUMERICAL METHODS IN ENGINEERING
Commun. Numer. Meth. Engng 2002; **18**:131–139 (DOI: 10.1002/cnm.475)

Control strategies for timestep selection in simulation of coupled viscous flow and heat transfer

A. M. P. Valli[1,*,†], G. F. Carey[2] and A. L. G. A. Coutinho[3]

[1]*Department of Computer Science, Federal University of Espírito Santo, Brazil*
[2]*CFD Lab, The University of Texas at Austin, Texas, U.S.A.*
[3]*Center for Parallel Computations, COPPE, Federal University of Rio de Janeiro, Brazil*

SUMMARY

This work investigates the use of control strategies for timestep selection and convergence rate improvement of non-linear iterative processes in the finite element solution of 2D coupled viscous flow and heat transfer. The present solution method employs a decoupled scheme, where the finite element flow formulation is based on a penalty Galerkin method and the heat transfer computations use a traditional Galerkin formulation. We compare the efficiency of the control strategies for timestep selection with another heuristic adaptive stepsize selection scheme. Numerical results for representative Rayleigh–Benard–Marangoni problems confirm that the non-dimensional kinetic energy could be a suitable parameter to improve the timestep selection when co-ordinated with the convergence control of non-linear iterations. We find approximate solutions with a much smaller number of steps without any significant loss of accuracy. Copyright © 2002 John Wiley & Sons, Ltd.

KEY WORDS: adaptive timestep control; control of non-linear iterations; finite element; Rayleigh–Benard–Marangoni flows

1. INTRODUCTION

Since the early 1970s there has been a rapid expansion of research and applications for finite element simulations of fluid flow and transport processes. With the evolution of the methodology and its extension to more complex classes of coupled problems there has been an increasing need for improved algorithms and other enhancements such as adaptive grid refinement. Several adaptive timestepping strategies have been studied as a means to provide stable accurate transient (and steady state) solutions more efficiently [1–4]. We remark that adaptive timestep selection can be viewed as examples of feedback control problems.

In the numerical integration of ordinary differential equations by implicit timestepping methods, a system of non-linear equations has to be solved at every step. In general, it is common to use fixed-point iterations or modified Newton iterations. In the present work, we use

*Correspondence to: Andrea Valli, Av. Fernando Ferrari s/n, Goiabeiras, Vitória 29060-900, ES, Brazil
†E-mail: avalli@inf.ufes.br

Received December 2000
Accepted September 2001

fixed-point iterations given by successive approximations. The convergence rate of the iterative methods depends on the stepsize [5], and the computational efficiency of the method can be measured by the total number of successive iterations to obtain the final solution. To improve efficiency, diminishing computational costs, it is necessary to control the convergence rate of the fixed-point iterations.

In the present study we propose two timestep control algorithms based on controlling accuracy or the convergence rate of the successive iterations. The objective of the stepsize control schemes is to minimize the computational effort to construct an approximate solution of a given problem in accordance with a desired accuracy. The algorithms look for changes in the key variables (velocities, pressure, temperature, etc.) or in the kinetic energy.

2. FORMULATION

We consider the transient flow of a viscous incompressible fluid as described by the Navier–Stokes equations coupled to the transport of heat by convection and conduction. Of particular interest in the present work is 2-D Rayleigh–Benard–Marangoni flows. Buoyancy and thermocapillary surface traction due to temperature gradients on the free surface provide the dominant forces driving these kind of flows. The dimensionless equations describing the Rayleigh–Benard–Marangoni flows are

$$\frac{\partial \mathbf{u}}{\partial t} + \mathbf{u} \cdot \nabla \mathbf{u} - \nabla^2 \mathbf{u} + \boldsymbol{\nabla} p = \frac{Ra}{Pr} T \mathbf{g} \tag{1}$$

$$\boldsymbol{\nabla} \cdot \mathbf{u} = 0 \tag{2}$$

$$\frac{\partial T}{\partial t} + \mathbf{u} \cdot \nabla T - \frac{1}{Pr} \nabla^2 T = 0 \tag{3}$$

where $\mathbf{u} = (u, v)$ is the velocity vector, p is the pressure, T is the temperature, Ra is the Rayleigh number, Pr is the Prandtl number and $\mathbf{g}$ is the gravity vector. Boundary conditions and initial conditions for temperature and velocities complete the mathematical statement of the problem. The non-dimensional boundary condition on the free surface is given by

$$\frac{\partial u}{\partial y} = -\frac{Ma}{Pr} \frac{\partial T}{\partial x} \tag{4}$$

where Ma is the Marangoni number.

Introducing a finite element discretization and basis on a uniform discretization Ω^h of rectangular elements, the direct approximation of the penalized variational formulation of the Navier–Stokes equations reduces to [6, 7]: for $\varepsilon > 0$, find $\mathbf{u}_h^\varepsilon \in V^h$ satisfying the initial condition with $\mathbf{u}_h^\varepsilon = \mathbf{u}_w$ on Γ_1^h such that

$$\int_{\Omega^h} \frac{\partial \mathbf{u}_h^\varepsilon}{\partial t} \cdot \mathbf{w}_h \, \mathrm{d}\Omega + \int_{\Omega^h} \mathbf{u}_h^\varepsilon \cdot \nabla \mathbf{u}_h^\varepsilon \cdot \mathbf{w}_h \, \mathrm{d}\Omega + \int_{\Omega^h} \nabla \mathbf{u}_h^\varepsilon : \nabla \mathbf{w}_h \, \mathrm{d}\Omega + \frac{1}{\varepsilon} \mathbf{I} (\nabla \cdot \mathbf{u}_h^\varepsilon)(\nabla \cdot \mathbf{w}_h) \, \mathrm{d}\Omega$$
$$= \int_{\Omega^h} \frac{Ra}{Pr} T \mathbf{g} \cdot \mathbf{w}_h \, \mathrm{d}\Omega - \int_{\Gamma_2^h} \frac{Ma}{Pr} \nabla T \cdot \mathbf{w}_h \, \mathrm{d}\Gamma \quad \text{for all } \mathbf{w}_h \in V^h \tag{5}$$

where **I** denotes reduced numerical integration, ε is the penalty parameter, $\Gamma^h = \Gamma_1^h \cup \Gamma_2^h$ is the finite element approximation of the boundary, Γ_1^h is the part of the domain that is not a free surface and Γ_2^h is the free surface. This leads to the following non-linear semidiscrete system of ordinary differential equations:

$$\mathbf{M}\frac{\mathrm{d}\mathbf{U}}{\mathrm{d}t} + \mathbf{s}(\mathbf{U}) + \mathbf{A}\mathbf{U} + \frac{1}{\varepsilon}\mathbf{B}\mathbf{U} = \mathbf{b}(\mathbf{T}) \tag{6}$$

which is solved by successive approximations in the present study. We integrate the ODE system implicitly using a Crank–Nicolson scheme, and the resulting linear systems are solved using a direct frontal solver.

Similarly, introducing a Galerkin finite element scheme for the temperature T

$$\int_{\Omega^h} \left(\frac{\partial T_h}{\partial t}\omega_h + \mathbf{u}\cdot\nabla T_h\omega_h + \frac{1}{Pr}\nabla T_h \cdot \nabla\omega_h \right) \mathrm{d}\Omega = 0 \quad \text{for all } \omega_h \in H_0^h \tag{7}$$

where we have assumed essential data for convenience. The resulting semi-discrete ODE system for the nodal vector **T** has the form

$$\mathbf{N}\frac{\mathrm{d}\mathbf{T}}{\mathrm{d}t} + \mathbf{C}(\mathbf{u})\mathbf{T} + \mathbf{D}\mathbf{T} = 0 \tag{8}$$

which is also integrated implicitly using the Crank–Nicolson scheme, and a frontal solver to find solutions of the resulting linear systems. The present algorithm employs a decoupled scheme, where the Navier–Stokes equations are solved first, in each timestep, lagging the temperature in the forcing term. Then, the energy equation is solved with the computed velocities as input. A single timestep for all equations is adaptively chosen using the control strategies described in the next section.

3. TIMESTEP CONTROL STRATEGIES

Stepsize selection algorithms in most integration methods are based on control of the maximum change in the key variables. According to Hairer and Wanner [8], stepsize selection can be viewed as an automatic control problem with a PID controller defined as

$$\Delta t_{n+1} = \left(\frac{e_{n-1}}{e_n}\right)^{k_\mathrm{P}} \left(\frac{1}{e_n}\right)^{k_\mathrm{I}} \left(\frac{{e_{n-1}}^2}{e_n e_{n-2}}\right)^{k_\mathrm{D}} \Delta t_n \tag{9}$$

where tol is some input tolerance, e_n is the measure of the change of the quantities of interest in time t_n, and k_P, k_I and k_D are the PID parameters.

We consider two different ways to measure the relative changes e_n. First, we use the changes in nodal velocities and temperature taking,

$$e_n = \max(e_u, e_T) \tag{10}$$

where

$$e_u = \frac{e_u^*}{\mathrm{tol}_u}, \quad e_u^* = \frac{\|\mathbf{u}^n - \mathbf{u}^{n-1}\|}{\|\mathbf{u}^n\|} \tag{11}$$

$$e_T = \frac{e_T^*}{\mathrm{tol}_T}, \quad e_T^* = \frac{\|\mathbf{T}^n - \mathbf{T}^{n-1}\|}{\|\mathbf{T}^n\|} \tag{12}$$

where tol_u and tol_T are user supplied tolerances. Second, we define e_n computing changes in the non-dimensional kinetic energy given by $K = \int_{\Omega^h}(u^{*2} + v^{*2})/2 \, \mathrm{d}\Omega$, where u^* and v^* are the non-dimensional velocity components. Now e_n is defined by

$$e_n = \frac{e_K^*}{\mathrm{tol}_K}, \quad e_K^* = \frac{|K^n - K^{n-1}|}{|K^n|} \tag{13}$$

where tol_K is a given tolerance.

Gustafsson and Söderlind [5] establish a model for controlling the convergence rate of the iterative non-linear solution method that relates the convergence rate to the stepsize. Assuming that the stepsize is limited by the convergence rate of non-linear iterations, the new stepsize should be chosen as

$$\Delta t_{n+1} = \frac{\alpha_{\mathrm{ref}}}{\alpha} \Delta t_n \tag{14}$$

where α_{ref} is a reference rate of convergence and α is an estimated rate of convergence. Now the controller tries to keep the estimated convergence rate as close as possible to a reference value. The estimated rate of convergence is calculated using three consecutive iterates for the velocities, $\mathbf{u}^{n-2}$, $\mathbf{u}^{n-1}$, and $\mathbf{u}^n$, as follows:

$$\alpha = \max \alpha_n = \max_n \frac{\|\mathbf{u}^n - \mathbf{u}^{n-1}\|}{\|\mathbf{u}^{n-1} - \mathbf{u}^{n-2}\|} \tag{15}$$

It is necessary to co-ordinate the convergence control algorithm (14) with the stepsize control strategy (9) so that efficiency is maintained.

We propose two timestep control algorithms based on controlling accuracy or the convergence rate of the successive iterations. The first control (Control 1) uses only the PID control for timestep selection, (9), with changes in velocities and temperature, (10), (11) and (12). In the second control (Control 2), the size of the timestep is limited by the changes in the kinetic energy or by the rate of convergence of the successive approximations. We take the minimum between the two values, $\Delta t_{n+1} = \min(\Delta t_r, \Delta t_\alpha)$, where Δt_r and Δt_α are defined by (9) and (14), respectively. Now, the relative changes e_n are calculated using (13). Computational cost of the selection procedures are negligible, since they involve only storing a few extra vectors, computation of norms and evaluation of kinetic energy.

Although feedback control theory provides sophisticated techniques to choose PID parameters, robustness is required when a general finite element method is used for a wide range of different simulations. We perform parametric studies of the PID controller in [2–4]. Numerical experiments demonstrate that the PID controller is very robust for all the applications studied here, and that we can adopt the following parameters: $k_{\mathrm{P}} = 0.075$, $k_{\mathrm{I}} = 0.175$ and $k_{\mathrm{D}} = 0.01$. Experimental studies will be given in the next section showing the efficiency of the two controls. Comparative studies between the two controls and the timestep selection strategy suggested by Winget and Hughes in Reference [1] will also be carried out for a representative test problem.

Table I. Comparison of specific results to benchmark case.

	Fixed Δt		Control 1		Control 2		Winget & Hughes		Benchmark	
Ra	Nu_0	ψ_{mid}	Nu_0	ψ_{mid}	Nu_0	ψ_{mid}	Nu_0	ψ_{mid}	Nu_0	ψ_{mid}
10^3	1.118	1.175	1.119	1.175	1.117	1.174	1.119	1.175	1.117	1.174
10^4	2.255	5.067	2.236	5.077	2.246	5.064	2.249	5.066	2.238	5.071
10^5	4.550	9.134	4.518	9.036	4.553	9.120	4.503	8.925	4.509	9.111

4. NUMERICAL RESULTS

The first case studied involves natural convection in a unit square with temperatures $T = 1, 0$ on the left and right walls, respectively, adiabatic top and bottom wall (no free surface), with $Pr = 0.71$ and different Rayleigh numbers, Ra, of 10^3, 10^4 and 10^5. The computed Nusselt number at the left wall, $Nu_0 = \int_0^1 q \, \mathrm{d}y$, where q is the heat flux, and the stream function at the midpoint, ψ_{mid}, are compared to benchmark computations [9]. We compare approximate solutions using fixed timestep sizes, Control 1, Control 2, the Winget and Hughes approach and the benchmark solution. The results are shown in Table I.

The approximate velocities and temperature are calculated using 9-node isoparametric quadrilateral elements in a uniform mesh of 16×16 elements at $Ra = 10^3$, 10^4 and 32×32 elements at $Ra = 10^5$. We assume that the steady-state occurs when the kinetic energy at two different timesteps reaches a relative difference less than a given tolerance, tol_{st}. The initial timestep size in all cases is chosen to have convergence of the successive iterations at the beginning of the process. If we start with a timestep size greater than the initial timestep defined below, the successive approximation iterations failed to converge after a few time steps. The results are in good agreement for all the cases, with percentage errors no more than 1 per cent in all quantities for Controls 1 and 2. However, observe that the differences increase as Ra increases due to the growing difficulty of the problem. The Winget and Hughes approach also produces good results with percentage errors no more than 2 per cent in all quantities. The stream function contours and temperature contours are shown in Figure 1.

Now we compare the computational effort to calculate the solution for $Ra = 10^3$. Since computational cost of the controls are negligible, the computational effort is measured by the total number of successive approximations needed to calculate the velocity field using one of the approaches divided by the number of successive approximations obtained using a fixed timestep size. We start with a minimum timestep size of 0.01, and we allow a maximum timestep size of 0.1. We define a tolerance of 0.1 for changes in nodal velocities and temperature, and a tolerance of 1.0 for changes in kinetic energy. The reference rate of convergence is equal to 0.2. We assume that the steady-state solution is reached when $\text{tol}_{\text{st}} = 10^{-4}$. We calculate the number of time iterations, ntstep, the number of rejected steps, nrejec, the total number of successive approximations, nsa, and the computational effort, c_{effort}. The results for $Ra = 10^3$ are shown in Table II.

We can observe in Table II that the number of successive approximations necessary to calculate the approximate solutions was reduced for all approaches. However, Control 2 presented the best results. We obtain the solution with 24 successive iterations using Control 2,

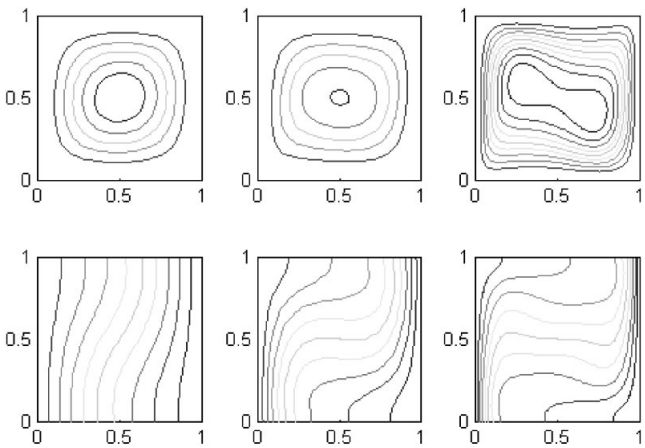

Figure 1. Stream function contours (top) and temperature contours (bottom) for $Ra = 10^3$, 10^4 and 10^5.

Table II. Computational effort for the natural convection problem, $Ra = 10^3$.

$Ra = 10^3$	ntstep	nrejec	nsa	c_{effort}
Fixed Δt	24	0	58	1
Control 1	11	0	32	0.55
Control 2	8	0	24	0.41
Winget and Hughes	15	0	41	0.71

and we need 58 iterations with the fixed timestep. Thus, we are able to calculate the solution 2.4 times faster using the Control 2 without any significant loss of accuracy. For Control 2, the choice of the timestep is dominated by the changes in the kinetic energy in all iterations. Figure 2 shows the timestep size against time and the number of successive approximations against time using Control 1, Control 2 and the Winget and Hughes approach for $Ra = 10^3$. In this example the kinetic energy is the most suitable parameter to choose the timestep, since Control 2 gives the best result. It is worthwhile noting also that Control 2 begins to act before any other approach and, after a few steps, provides a timestep equal to the maximum stepsize allowed, 0.1.

The second numerical experiment involves buoyancy forces due to temperature gradients and thermocapillary forces caused by gradients in the surface tension. The flow domain and boundary conditions are the same as in the first example, except that the top is now a flat free surface. The Rayleigh number is 10^3, the Prandtl number is 0.71, and the problem is solved at different Marangoni numbers. The approximate steady-state velocities and temperature are calculated using biquadratic elements in a uniform mesh with size $h = \frac{1}{16}$. Here we assume that the steady-state occurs when $\|\mathbf{u}^n - \mathbf{u}^{n-1}\| < \tau_u \|\mathbf{u}^n\|$ and $\|\mathbf{T}^n - \mathbf{T}^{n-1}\| < \tau_T \|\mathbf{T}^n\|$, where n denotes the timestep index, $\|\cdot\|$ denotes Euclidean norm, and τ_u and τ_T are input tolerances.

We find solutions at $Ma = 1$, 100 and 1000 (see Figure 3). At $Ma = 1$, the effect of the surface tension is small and the streamlines are roughly circular. The solution is similar

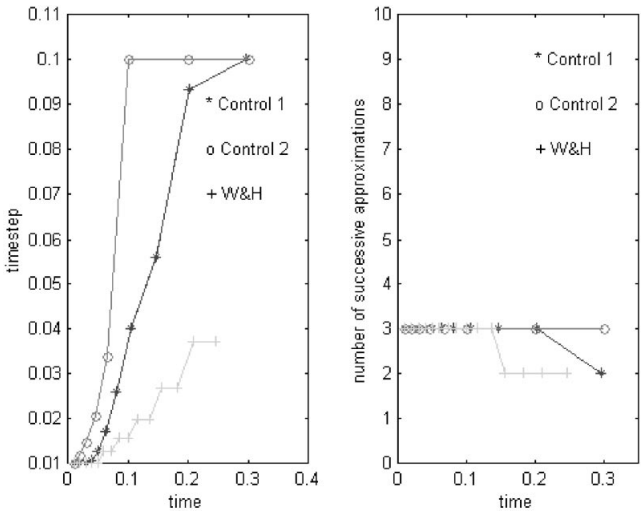

Figure 2. Timestep variation (left) and number of successive approximations (right) using Controls 1, 2 and the Winget and Hughes approach for $Ra = 10^3$.

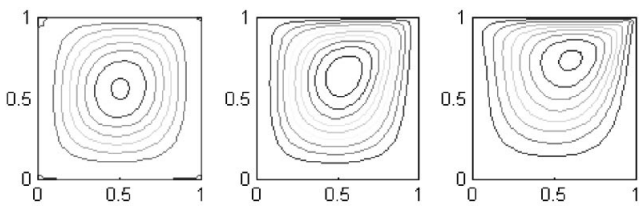

Figure 3. Stream function contours for $Ma = 1,\ 100$ and 1000.

in structure to the classic buoyancy driven flow studied in the first example, Figure 1. At $Ma = 100$, the effect of the thermocapillary force at the free surface is more pronounced. The streamlines are concentrated near the top boundary. At $Ma = 1000$, the flow is being strongly driven at the top boundary as seen in similar experiments presented by Zebib *et al.* [10].

To study the behaviour of the PID timestep selection in the second problem, we select the case where $Ma = 100$. The steady-state solution is obtained at $\tau_u = 10^{-3}$ and $\tau_T = 10^{-4}$. We start with a minimum timestep size of 0.001, and we allow a maximum timestep of 0.1. Solutions are obtained with tolerances of 0.2, 0.1 and 1.0 for changes in nodal velocities, temperature and kinetic energy, respectively. The reference rate of convergence is equal to 0.2. As we can see in Table III, we obtain the solutions with 57 successive approximation iterations using Control 2. With a fixed timestep size of 0.001, we need 272 iterations. Thus, the solutions are obtained 4.8 times faster using Control 2. Here, the choice of the timestep in Control 2 is dominated by the changes in the kinetic energy, with only three time iterations limited by the changes in the convergence rate of the successive iterations.

Table III. Computational effort for the Rayleigh–Benard–Marangoni problem, $Pr = 0.71$, $Ra = 1000$ and $Ma = 100$ in a unit square.

Case	ntstep	nrejec	nsa	c_{effort}
Fixed Δt	118	0	272	1
Control 1	23	0	75	0.28
Control 2	13	0	57	0.21
Winget and Hughes	25	0	80	0.29

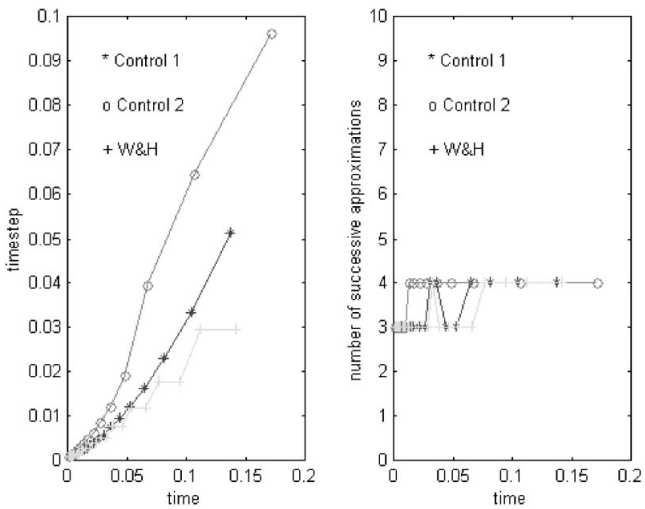

Figure 4. Timestep variation (left) and number of successive approximations (right) using Controls 1, 2 and the Winget and Hughes approach for $Pr = 0.71$, $Ra = 1000$ and $Ma = 100$ in a unit square.

Figure 4 shows the timestep variation and the number of successive approximations against time using Controls 1, 2 and the Winget and Hughes approach. We can observe that Control 1 yields a smoother sequence of time steps than the Winget and Hughes approach. However, these two approaches are equivalent in terms of efficiency. Control 2 calculates the solutions with the smallest computational effort.

5. CONCLUSIONS

Based on numerical studies of representative Rayleigh–Benard and Rayleigh–Benard–Marangoni problems, it is concluded that we find approximate solutions with a smaller number of steps without any significant loss of accuracy. In addition, the controllers also produce a smooth variation of timestep, suggesting that a robust control algorithm is possible. Further, the control strategy that maintains the desired solution accuracy by adjusting the timestep size to account for changes in the kinetic energy or by the rate of convergence of the successive approximations showed the best results in all cases studied here.

REFERENCES

1. Winget JM, Hughes TJR. Solution algorithms for nonlinear transient heat conduction analysis employing element-by-element iterative strategies. *Computational Methods in Applied Mechanics and Engineering* 1985; **52**:711–815.
2. Valli AMP, Carey GF, Coutinho ALGA. Finite element simulation and control of nonlinear flow and reactive transport. In *Proceedings of the 10th International Conference on Finite Element in Fluids*, Tucson, Arizona, 1998; 450–455.
3. Valli AMP, Coutinho ALGA, Carey GF. Adaptive control for time step selection in finite element simulation of coupled viscous flow and heat transfer. In *European Conference on Computational Mechanics*, Munchen, Germany, August 1999.
4. Valli AMP, Coutinho ALGA, Carey GF. Adaptive stepsize control strategies in finite element simulation of 2D Rayleigh–Benard–Marangoni flows. In *15th Brazilian Congress on Mechanical Sciences*, Águas de Lindóia, SP, Brazil, November 1999.
5. Gustafsson K, Söderlind G. Control strategies for the iterative solution of nonlinear equations in ODE solvers. *SIAM Journal of Scientific Computing* 1997; **18**(1):23–40.
6. Carey GF, Oden JT. *Finite Elements*: *Fluid Mechanics*, vol. 6. Prentice-Hall: Englewood Cliffs, NJ, 1986.
7. Carey GF, Krishnan R. Penalty finite element methods for the Navier–Stokes equations. *Computer Methods in Applied Mechanics and Engineering* 1984; **42**:183–224.
8. Hairer E, Wanner G. *Solving Ordinary Differential Equations II*: *Stiff and Differential-Algebraic Problems*. Springer: Berlin, 1993.
9. De Vahl Davis G. Natural convection in a square cavity: a comparison exercise. *International Journal for Numerical Methods in Fluids* 1983; **3**:227–248.
10. Zebib A, Homsy GM, Meiburg E. High Marangoni number convection in a square cavity. *Physics of Fluids* 1985; **28**(12):3467–3476.

